



XA0300585

Seismic Fragility Analyses

by: M. Kostov

SEISMIC FRAGILITY ANALYSES
(Case Study)
Marin Kostov

1. Introduction

In the last two decades there is increasing number of probabilistic seismic risk assessments performed. The basic ideas of the procedure for performing a Probabilistic Safety Analysis (PSA) of critical structures (NUREG/CR-2300, 1983) could be used also for normal industrial and residential buildings, dams or other structures. The general formulation of the risk assessment procedure applied in this investigation is presented in Franzini, et al., 1984. The probability of failure of a structure for an expected lifetime (for example 50 years) can be obtained from the annual frequency of failure, β_E , determined by the relation:

$$\beta_E = \int [d[\beta(x)]/dx] P(f|x) dx \quad (1)$$

$\beta(x)$ is the annual frequency of exceedance of load level x (for example, the variable x may be peak ground acceleration), $P(f|x)$ is the conditional probability of structure failure at a given seismic load level x . The problem leads to the assessment of the seismic hazard $\beta(x)$ and the fragility $P(f|x)$.

The seismic hazard curves are obtained by the probabilistic seismic hazard analysis. The fragility curves are obtained after the response of the structure is defined probabilistically and its capacity and the associated uncertainties are assessed. Finally the fragility curves are combined with the seismic loading to estimate the frequency of failure for each critical scenario. The frequency of failure due to seismic event is presented by the scenario with the highest frequency.

2. Basic Formulation of Fragility Curve Model

The fragility of a structures is defined as the conditional probability of failure at a given value of seismic response parameter as maximum acceleration, velocity displacement, spectral acceleration, effective acceleration Arias intensity, etc. Generally there are two ways of defining seismic fragilities, i.e. in terms of global ground motion parameter or in terms of local response parameter.

Most frequently the objective of the fragility evaluation is to estimate the peak ground motion acceleration value for which the seismic response of a structure (system, component) exceeds the capacity resulting in failure. The estimation of the ground acceleration value could be performed on the base of calculations or based on experience data (the later could be from real earthquakes or dynamic tests). Because there are many sources of variability the structure (component) fragility is expressed usually by family of curves. A probability value is assigned to each curve to reflect the uncertainty in the fragility estimation (fig.2.1).

The first step in generation fragility curve is a clear definition of what constitutes failure for the analyzed object. The failure definition may differ significantly depending of the goals of the analysis, e.g. failure could be any loss of function, strength, integrity, value, etc. One and the same failure may happen in different failure modes, each of them have to be clearly identified and addressed. A post office may fail for instance due to structural failure, failure in the electrical supply, failure of the road system, failure of the communication equipment, failure of the auxiliary facilities. etc. Another example of failure mode differentiation is the ductile or the brittle mode of failure. If there is clear definition for the possible failure modes, fragility has to be developed for the mode which is most likely to occur. otherwise fragilities have to be developed for each identified mode.

One simple but effective fragility model supposes that the entire family of curves representing a particular failure mode can be expressed by median ground acceleration A_m and two random variables ϵ_R and ϵ_U , thus the ground acceleration capacity A is given by

* Associate Professor, Dr., Head of Department "Seismic Mechanics", CLSMEE, Bulgarian Academy of Sciences

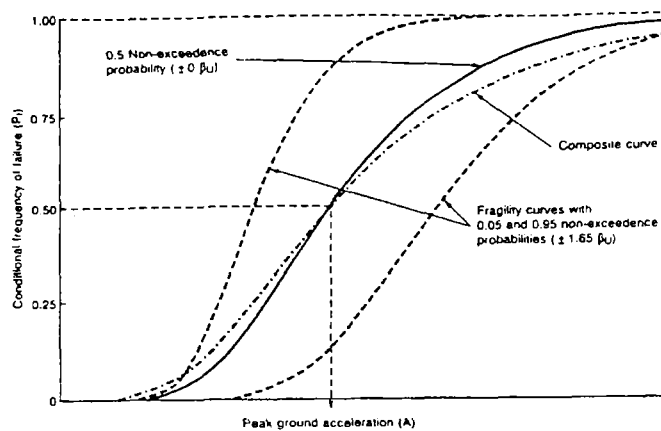


Fig.2.1 Seismic fragility family curves

$$A = A_m \cdot \varepsilon_R \cdot \varepsilon_U$$

ε_R and ε_U are log-normally distributed with unit medians and standard deviations β_R and β_U respectively. They represent the inherent randomness about the median and the uncertainty of the median value respectively. In some cases the composite variability β_c is used, defined by:

$$\beta_c = (\beta_R^2 + \beta_U^2)^{1/2}$$

The use of β_c and A_m provides a single best estimate fragility curve which does not explicitly separate randomness from uncertainty.

In estimating the fragility parameters it is convenient to use an intermediate random variable, called factor of safety, F . The factor of safety is defined as:

$$F = (\text{Actual seismic capacity}) / (\text{Actual response due to DE})$$

DE is the design earthquake

Further on the factor of safety can be expressed by:

$$F = F_S \cdot F_\beta \cdot F_{RS}$$

F_S is called stress factor, representing the ratio of the ultimate strength to the stress, calculated for DE.

F_β is the inelastic energy absorption factor, which depends on the available ductility and reflects the ability of the structures to withstand seismic loads beyond yield without loss of function.

F_{RS} is the structural response factor that recognizes that in the design the structural response have been computed using specific (some times conservative) response parameters. The response factor is modeled as a product of factors influencing the response variability, e.g. spectral shape factor (representing the variability of the ground motion), damping factor (representing the variability of response due to difference of the actual damping and design damping), modeling factor accounting for the uncertainties due to modeling assumptions, mode combination factor, earthquake component combination factor, factor to reflect the reduction of the seismic motion with depth, factor to account for soil-structure interaction effects, etc.

The median and logarithmic standard deviation of the safety factor F are expressed as:

$$mF = mF_S \cdot mF_\beta \cdot mF_{RS}$$

and

$$\beta_F = (\beta_S^2 + \beta_\beta^2 + \beta_{RS}^2)^{1/2}$$

The logarithmic standard deviation could be further divided into random variability and uncertainty. The median factor of safety multiplies the design ground acceleration to obtain the median ground capacity.

3. Case 1. Concrete Gravity Dam

The probability of seismically induced failure of large concrete dams is of special importance because of the potential flood due to the released water from the lake. The need of such assessment arises moreover in the case where the design values of existing large dams differ from the design values specified by new standards. The basic steps of the procedure are: assessment of the seismic hazard and uncertainties; statistical formulation of material properties and loading; assessment of statistics of the response; definition of the failure criteria; evaluation of the probability of failure. The case presented hereafter is on Antonivanovzi dam which is located in the south-west part Bulgaria. The dam safety is not related to the nuclear facilities in Bulgaria and is presented only as an example.

3.1 Seismic hazard analysis of the dam site

The seismic hazard curves result from the application of probabilistic models of the site region defined on the basis of complex analyses including description of regional tectonic, review of historic seismicity, identification of seismic source zones, development of earthquake recurrence relationships. The models incorporate the following main characteristics:

there are no contemporary active faults which pass through the dam and the dam reservoir.

Four potential foci zones have been identified in the near field (30km) zone around the dam site which might generate earthquakes with maximum magnitude from 5 to 7. The events with magnitude 7 are generated in a depth 10km to 20km. Earthquakes with magnitudes greater than 7 have occurred at a distance of about 60km from the site and events with $M \geq 6$ - over 40km. At shorter distances the events occurred are with $M_{max} < 6$. In the region there are five epicentral zones in the territory of Bulgaria and one in the North part of Greece. The strongest seismic event is realized in the Marica zone on the territory of Bulgaria. The possible effects from Vrancea zone situated at a distance of more than 400km from the dam site are also studied.

The ground motion attenuation relationships used for the models are based on the analysis of strong motion data records from earthquakes in the Balkan region countries, Italy, USA.

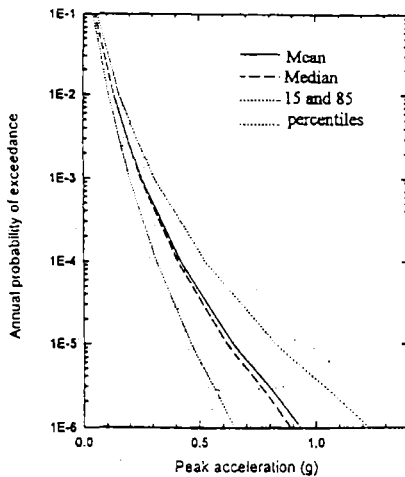


Fig. 3.1 Mean, Median 15 and 85 percentiles Hazard curves

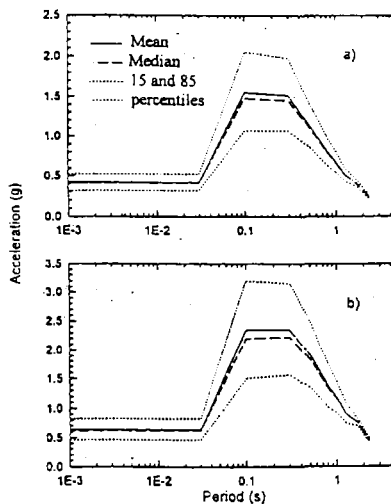


Fig. 3.2 Hazard Response spectra, 5% damping, anual probability of exceedance: a) 10^{-4} ; b) 10^{-5}

The following uncertainties in the mathematical model are considered: configuration of the seismic sources, uncertainty in spatial distribution of seismicity (for the Marica epicentral zone), uncertainty of focal depth, uncertainty in maximum expected magnitude, different alternatives of the acceleration attenuation law, and uncertainty of law dispersion. As a result for the Antonivanovtsi dam site 72 hazard curves are obtained..

In Figure 3.1 are presented the mean, median, 15th-percentile and 85th-percentile hazard curves obtained from the calculated total hazard assuming lognormal distribution of the peak acceleration at a given annual probability of exceedance.

In a similar way the equal hazard response spectra for four hazard levels A, B, C and D, with annual probability of exceedance 0.01, 0.001, 0.0001, 0.00001, respectively, are obtained.. In Figure 3.2 are shown the equal hazard response spectra for levels C and D.

3.2 Statistical formulation of material properties and loading

Strength and elastic properties

The materials of the dam structure are identified into 8 types: 5 of them are for the concrete of the dam body and 3 - for the rock foundation. For each type of material the mean value and the variation coefficient of the material characteristics (static and dynamic compression, tensile and shear strength, and the elastic module) are determined based on in situ and lab tests.

Thermal loads

The thermal loads are represented by sets of nodal temperature differences. For this 2D linear transient heat transfer analysis) is performed with input data obtained on the basis of statistical meteorological observations.

The values of the hydrostatic, hydrodynamic and filtration pressure are function of the water level in the lake. The maximum working water level of Antonivanovtsi dam is 535.8m and the minimum level is 505m. An uniform distribution is assumed for the water levels between 535.8m and 505m.

The seismic load is the most important for the seismic risk analysis.

For each seismic hazard level (A, B, C and D) the seismic loading is presented by a set of acceleration response spectra and the corresponding acceleration time histories. Those spectra are generated on the base of the statistics of the equal hazard spectra obtained by the seismic hazard analysis.

Each one of the generated spectra is used as a target spectrum for generation of acceleration time histories (three statistically independent generations representing three components - two horizontal H1 and H2 and one vertical V). The maximum accelerations of the vertical components are obtained from the horizontal ones by scaling with random numbers with mean value of 0.5 and standard deviation of 0.3.

3.3. Assessment of the response statistics

Finite Element Model

A 2D finite element model of the highest block of the dam structure is used in the analysis. A plane strain condition is assumed. The rock foundation and the concrete dam body are modelled. The model length is 450m, the height of the rock foundation is 206m and the total model height is 340m. Along the rock base boundaries the model is fixed. The rock foundation is assumed massless in the analyses.

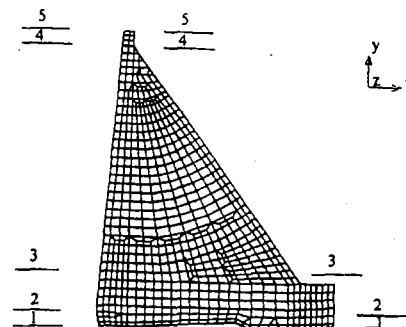


Fig. 3.3 Location of sections

Four cross sections are investigated in details. Their location is shown in Figure 3.3. The sections are as follows: base joint - section 1; injection gallery - section 2; control gallery - section 3; crest zone - section 4.

Computational Procedure

The deterministic analyses are carried out according to the computational procedure based on an advanced Monte Carlo method (Latin Hypercube Experimental Design, LHCED) for simulation. The main steps of the computation are as follows:

1. Preparation of input variable samples by Latin Hypercube Experimental Design procedure.
2. Computation of stresses due to static loads.
3. Computation of eigen values and modes of vibrations.
4. Evaluation of stresses due to seismic loads.
5. Stress superposition.
6. Computation of maximum stresses.
7. Statistics of the results.

Applying the LHCED procedure (Iman & Conover., 1981) sets of the input variables contributing to the response of the dam structure are prepared. In the case of the Antonivanovtsi dam for each variable a stratified sample of size 10 is prepared. The input parameters that are varied in this study are the strength and elastic properties of the dam structure and foundation rock; thermal loading; hydrostatic, hydrodynamic loading, filtration pressure - correlated with the water level in the reservoir; material damping; natural frequency of the structure vibrations; seismic excitation.

The seismic loading is represented by 10 acceleration response spectra and 10 accelerograms for each seismic level A, B, C and D. The spectra are generated on the base of the mean equal hazard spectra obtained by the seismic hazard analysis. Lognormal distribution of the spectral values is assumed.

The response spectra of the generated acceleration time histories are computed and statistically processed for each safety level. Their mean values and standard deviations are compared with the mean spectrum of equal hazard and the respective standard deviation. As an illustration a comparison for seismic level C is shown in Figure 3.4.

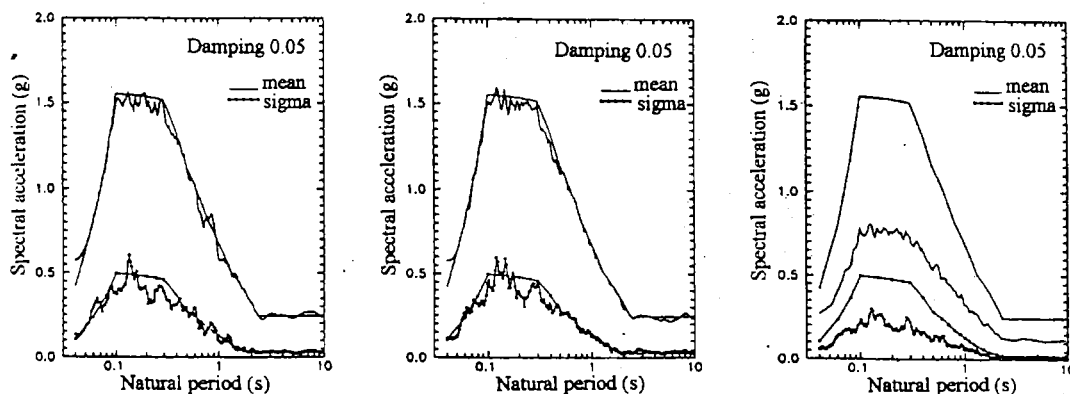


Fig. 3.4 Equal hazard spectra and spectra of generated accelerograms, annual probability of exceedance 10^{-4} , components: H1; H2; V

The procedure is applied for each of the accepted four levels with annual probability of exceedance 10^{-2} (level A), 10^{-3} (level B), 10^{-4} (level C), and 10^{-5} (level D).

The results for each safety level are processed separately. The response parameters studied in the probabilistic analysis are the normal S_{yy} stress, the tangential S_{xy} stress and the tensile zone length.

Statistics of results

For the statistical processing of the response a normal distribution of response parameters is assumed. In Figure 3.5 is shown the cumulative distribution functions (CDF) of S_{yy} in nodal point 73 (the corner of the base joint-upstream face) for safety level B. The stars in this figure present the computed values and the line shows the theoretical normal CDF. The computed values fit well the accepted normal CDF and allow to assess the statistical character of the investigated parameters.

The mean values and the standard deviation of the generated response quantities are estimated for each nodal point of the investigated sections. For illustration in Figure 3.6 are shown the mean value and the standard deviation of S_{yy} for section 2. The mean values and the respective standard deviation of the tensile zone lengths of the four sections for all seismic loading levels are computed as well.

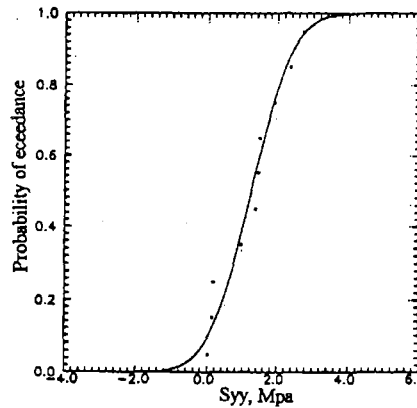


Fig. 3.5 Cumulative distribution function SYy, NP 73, level B

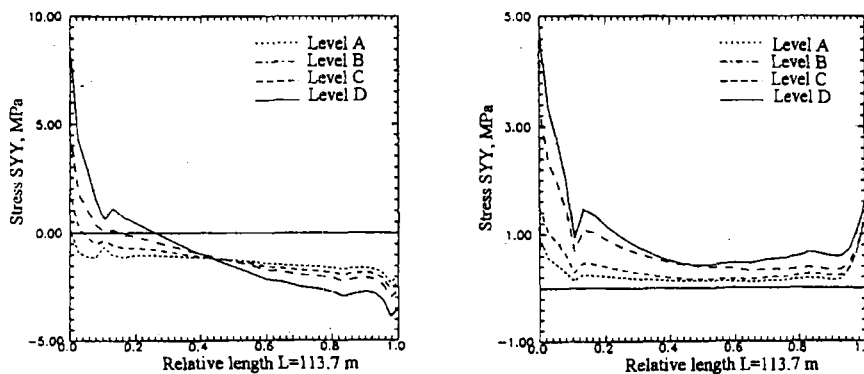


Fig. 3.6 Statistics of stresses, section 2: a) mean SYy, b) standart deviation SYy

Scenarios of failure due to seismic excitation

To assess the probability of failure the following scenarios for failure are considered:

1. Exceedance of the concrete tensile strength. This is the most common case for failure of concrete dam structures. In the base joint (section 1) two additional cases are investigated. For this section the scenarios are:

- a) Probability for exceedance of the concrete tensile strength (above the foundation joint),
- b) Probability for exceedance of the rock base tensile strength (below the foundation joint),

2. Exceedance of the allowable length of tensile zone. This scenario is defined because of the requirements of the norms for design of concrete gravity dam. It is related to the possibility of failure due to large tensile stresses as well as to the control of pressure stresses. The mean value of the allowable tensile zone is accepted conservatively as follows: 10% of the length of base joint and 20% of the length of all other sections, and the variation coefficient is 20% (Norms, Concrete and reinforced dams, 1986).

3. Probability of failure from simultaneous exceedance of the tensile strength and the allowable length of tensile zone. For the base joint two additional cases are investigated:

- a) Probability of failure from simultaneous exceedance of the concrete tensile strength and the allowable length of tensile zone,
- b) Probability of failure from simultaneous exceedance of the rock tension (below the base joint) and the allowable length of tensile zone,

4. Probability for loss of stability due to sliding in the concrete-rock contact.

The most important scenarios from engineering point of view are scenarios 3 and 4.

For each scenario two alternatives are considered. The first alternative is when the maximum stresses are used in the analysis. That implies full correlation of damages in adjacent nodes, i.e. if there is a damage in one node all other nodes would be also damaged. This assumption is very conservative. The second alternative is when averaged stresses are used in the analysis. This means the tensile stresses to be determined in a small zone, i.e. some correlation between the behaviour of adjacent elements to be accepted.

Conditional probability of failure due to seismic events

The probability of failure expressed by the probability of exceedance of the tensile strength in each node of the FE mesh within the investigated section is computed under the assumptions that the stresses and the resistance (strength) are normally distributed.

The conditional probability of failure is computed by the expression:

$$P_f = \int \beta FR(x) f_L(x) dx \tag{2}$$

where $FR(x)$ is the distribution function of the resistance and $f_L(x)$ is the density function of the seismic loading distribution.

3.4. Risk assessment

The total probability of failure is determined by integration of the seismic hazard curves together with the fragility curves. The LHCED procedure is applied for the integration..

The fragility curves are obtained from the computed discrete values of the conditional probabilities for each seismic level. For this purpose the function that passes through those discrete values is approximated with cumulative log-normal distribution functions. The approximation is done by the least square method. The procedure is performed for each seismic level and each section (for 50% and 85% confidence level). For example, in Figure 3.7 the curves are shown for scenario 1, first alternative (maximum stresses), section 1 (base joint). The solid line represents the curve of the mean values of the conditional probability, the stars are the discrete values. On the basis of the approximation function characteristics 10 fragility curves for each scenario and section are generated with mean value and standard deviation corresponding to the values obtained by the numerical experiment..

In Figure 3.8 are shown for scenario 3b the distributions of the total probability of failure in dependence on the acceleration. The figure illustrates also the way of integration. Each ordinate gives the contribution of the respective acceleration to the total probability. The total probability distribution shows that the seismic loading levels for which the analysis is performed are selected correctly. In section 1 accelerations higher than 0.4g have small contribution.

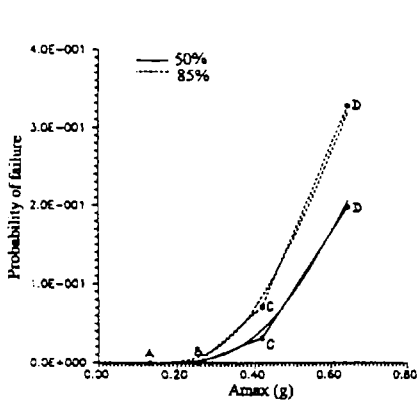


Fig.3.7 Approximation of the numerical generation Results for level A, B, C, D with log-normal CDF Cross section I, max SYY

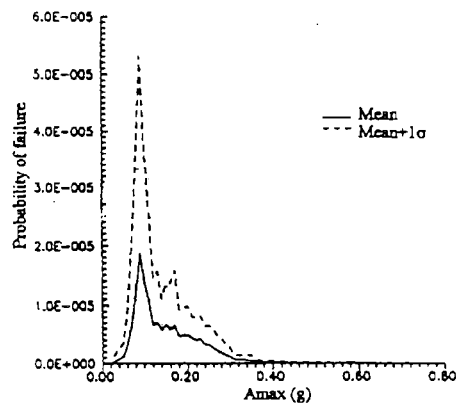


Fig. 3.8 Distribution of the total probability of failure depending on Amax; scenario 3b, section 1, maximum stress

The highest probability of failure is in the base joint resulting from simultaneous exceedance of the rock tensile strength and the allowable tensile zone length. From all considered sections the most affected is the section 1 - base

joint and section 2 - injection gallery. In these section the total probability of failure for a period of 50 years is defined and the values are given in Table 3.1.

Table 3.1 Total probability of failure for 50 years

Scenario	Probability of non-exceedance		
	15% confidence level	50% confidence level	85% confidence level
Failure from simultaneous exceedance of the tensile strength in the rock and the allowable length of tensile zone	3.49E-03	7.69E-03	1.69E-02
Failure from simultaneous exceedance of the concrete tensile strength and the allowable length of tensile zone - section 2	4.10E-04	1.00E-03	2.45E-03

Sensitivity analysis

The sensitivity of the results when the input parameters (strength characteristics of materials, variation of seismic hazard, of stresses, etc.) are varied and the influence of the size of parameter samples on the probability are investigated.

Thus the probability of failure in the base joint can be reduced by decreasing the tensile stresses, by increasing the tensile strength in the rock or by decreasing the central seismic hazard values. These three factors can be used also in combination with the purpose of reducing the seismic risk. By 50% variation of each one of those factors the most considerable effect on the seismic risk reduction is achieved. By the reduction of the tensile stresses the probability of failure decreases 29 times. By reduction of the central seismic hazard values the risk reduces 6.27 times and by the increase of the tensile strength of the rock the risk reduces 1.79 times.

4. Case 2. Steel frame industrial building

The steel frame industrial building analysis presented is part of a probabilistic safety analyses of a nuclear power plant. The building is an existing one, it is not safety relevant, but is important for electricity production. The outcomes of the probabilistic analysis have been the bases for a consequent seismic upgrading project. The probability of failure before and after upgrading respectively is used as measure for the upgrade effectiveness.

4.1. Structure description

The structure is a 2 bay steel frame. The first span is 45m and with a height of 38m and the second span is 12 m with a height 42m. In longitudinal direction the steel columns are placed in 3 rows (A, B, C) and 12 transversal axes (12m between two adjacent axes). They are connected by longitudinal hinged beams. Diagonal bracing provides the longitudinal stiffness. The foundations are single footings. The roof structure is steel truss.

Next to the steel building there is a reinforced concrete building. It is also frame structure (one bay, 12 m span). Because of the small gap between the two buildings as well as due to the common foundation used in row C the two buildings are analyzed together in order to account for the structure to structure interaction.

4.2. Modeling and Analyses

A comprehensive 3-dimensional FE model has been developed for all essential structural elements. The soil-structure interaction is accounted by equivalent spring and dashpots, connected to each footing. The seismic excitation is defined by a maximum acceleration for 10^{-3} annual probability of exceedance and a site specific broad band design spectrum. Modal analysis and time history integration are used for the dynamic analyses. Some of the important mode shapes are presented in fig. 4.1. Static analyses for all design load combinations are performed also. Most unfavorable loading condition is found out and capacity estimation for all bearing elements is performed respectively. The results of the analyses are showing that:

1. All columns have sufficient bearing capacity and can withstand the design seismic motion.
2. The column-roof connection has insufficient capacity and bad detailing. Failure of the roof structure is a possible failure scenario.
3. The longitudinal beams and X-bracings are very slender and failure due to overloading is possible.
4. The safety of the foundation for sliding and overturning is guaranteed.

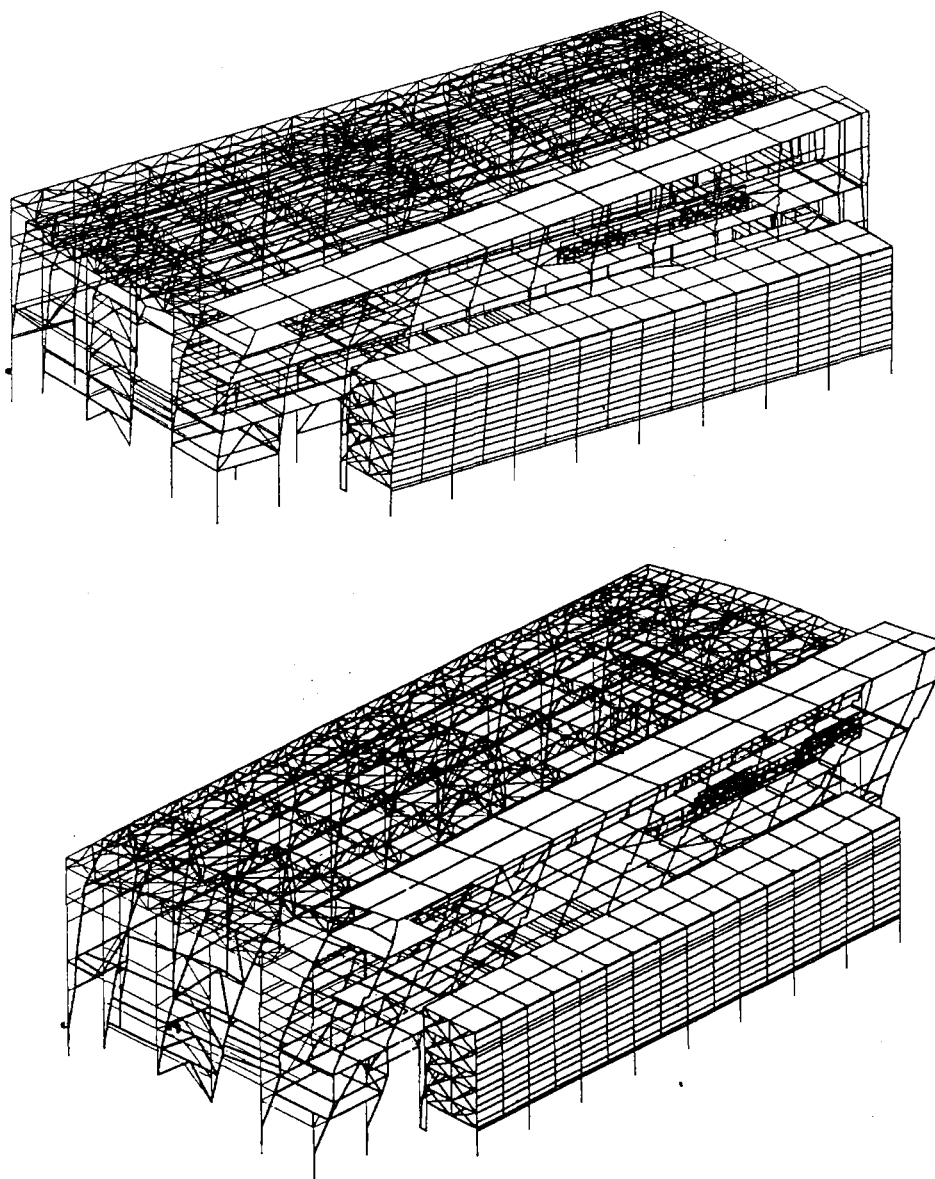


Fig. 4.1 Important mode shapes

Those conclusions mean that there are at least 4 scenarios with considerable influence on the overall structural safety that have to be analyzed. For each scenario a fragility curve is developed following the methodology described in section 2 above.

In order to improve the safety an upgrading concept has been proposed. It consist of improving of the column-roof connection by using a better detailing and reducing of the slenderness of the longitudinal beams and x-bracing by

increasing the sections of the members or additional support points (shortening of buckling length). Fragility analyses are performed also for the upgraded structure and results are compared with the existing structure.

4.3. Fragility curves, Failure probability assessment

As explained in the beginning the fragility curve is assumed log-normal. The mean failure acceleration is determined by scaling the design acceleration by the factor of safety. As also explained the factor of safety can be represented as product of different partial safety factors. For the present analysis the following partial safety factors are used:

$$F = F_S \cdot F_\beta \cdot F_{RS}$$

Where

$$F_{RS} = F_M \cdot F_C$$

F_M is safety factor representing the conservatism of the modeling.

F_C is safety factor representing the conservatism of the member force combination procedure.

Similarly the variations β_R and β_u are determined for each partial safety factor.

As an example the values for the determination of the fragility curve for roof failure are presented below:

Table 4.1. Partial safety factors and corresponding uncertainties

Safety Factor	Mean	β_R	β_u
F_S	1.050	0.100	0.150
F_β	1.400	0.050	0.100
F_M	1.100	0.050	0.050
F_C	1.100	0.050	0.050
F	1.791	0.132	0.193

The mean maximal acceleration that will cause failure is determined as $A_m = 0.1 \cdot 1.791 = 0.179g$. The corresponding fragility curve is shown in fig. 4.2.

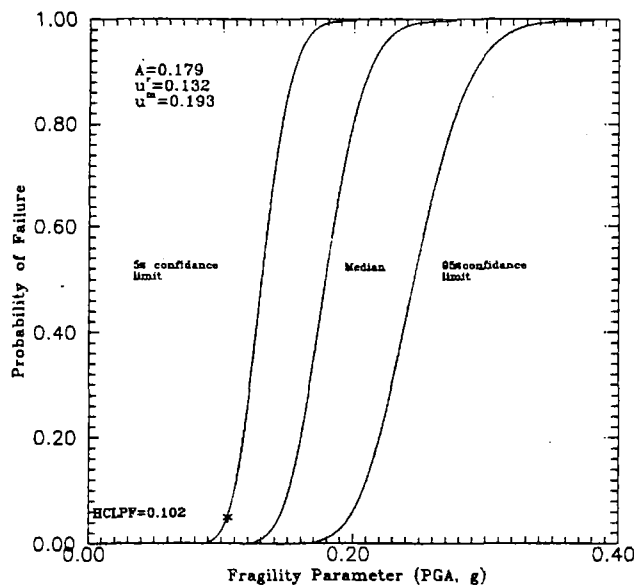


Fig. 4.2 Fragility curves

A summary for all considered failure modes before and after upgrading are presented in table 4.2.

Table 4.2. Fragility curve characteristics

Failure Mode	Before Upgrading			After Upgrading		
	A_m	β_R	β_u	A_m	β_R	β_u
Roof failure	0.179	0.132	0.193	0.356	0.132	0.193
Bracing failure– row A	0.125	0.132	0.193	0.404	0.132	0.226
Bracing failure– row B	0.147	0.132	0.193	0.390	0.132	0.226
Bracing failure– row C	0.154	0.132	0.193	0.396	0.132	0.226

For the site of that building there are seismic hazard curves for maximal acceleration developed. The methodology uses is the same as described in case 1. The fragility curves and the hazard curve are integrated together and the annual probability of failure is determined for each failure scenario. The results are presented in table 4.3 for 85% confidence limit.

Table 4.3. Probability of failure (85% confidence level)

Failure Mode	Before Upgrading	After Upgrading
	Probability of failure	Probability of Failure
Roof failure	1.242E-3	2.356E-5
Bracing failure– row A	7.872E-3	1.518E-5
Bracing failure– row B	3.548E-3	1.886E-5
Bracing failure– row C	2.836E-3	1.717E-5

5. Case 3. Soil Liquefaction

There are big number of liquefaction analysis methods. Most of them are based on statistical observations. Unfortunately there are rear confidence limits and uncertainties reported for the respective method. In the presented case analysis a site was initially assessed deterministically using several methods. Some of the methods were assessing the site as potentially liquefiable, some were saying that the site is safe. The characteristics of the site are presented in table 5.1. For example the simplified Seed method (1971) is saying that the site will liquefy. The Seed method based on SPT values (1979) is saying that the site is almost on the boundary, i.e the safety factor is generally more than 1, but is not definitely safe. The Seed method (1979) based on SPT and experimentally determined shear stress ratios (3 axial tests) is saying that the site is safe. The pore pressure generation analysis (Seed 1976) is also saying that the site is safe.

Table 5.1 Site characteristics

Layer No	Material	Thickness	Weight density	Relative density	SPT (N)	Permeability
		m	t/m ³	%	N	cm/s
1 *)	Sandy loes	8.6-10.5	1.9-2.1	-	-	
2	Loes-clay	1.7-3.5	1.9-2.1	-	-	
3	Fine sand	0.5-3.0	1.6-1.7	53	9/21	4*10 ⁻⁴
4	Fine sand	0.5-4.7	1.6-1.7	44	9/21	4*10 ⁻⁴

*) There is an overburden of 240 kPa on that layer.

For that site probabilistic analysis has been performed. The analysis scheme is similar to the one presented in case 1-dam analysis. There are only different methods used to assess the safety, i.e. for the dam assessment multiple stress analyses have been performed, for the liquefaction assessment multiple analyses based on the Seed (1979) method are performed.

The safety factor for liquefaction is expressed according to Seed (1979) as:

$$FS = SR/L$$

The SR is the cyclic stress ratio for equivalent number of cycles N_e (soil resistance) and L is the stress ratio caused by the equivalent number of cycles by an earthquake (seismic load). The experimentally determined cyclic stress ratio to generate liquefaction for the site is presented in fig. 5.1.

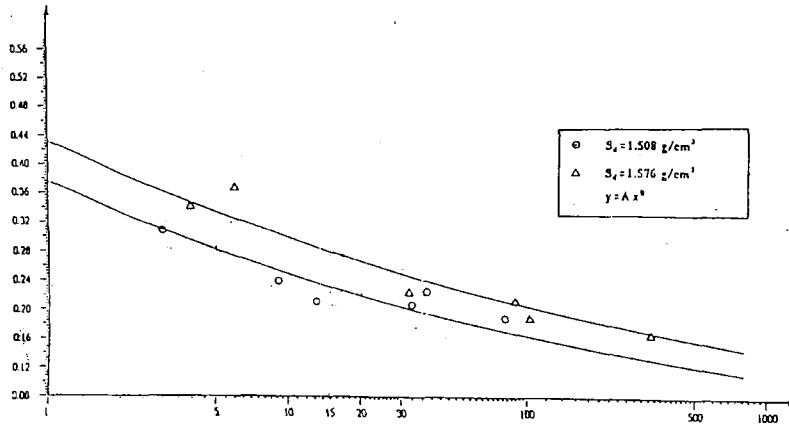


Fig. 5.1 Experimentally determined cyclic stress ratio

Because of the importance of the equivalent number of cycles of the earthquake excitations an additional simplified statistical analyses was performed to assess the site-specific excitation cycles. The site is located in the northern part of Bulgaria. The seismic hazard is governed by two type of seismic sources: local shallow sources with maximum magnitude up to 5.5 and fare field intermediate depth Vrancea source with maximum magnitude up to 7.5. The shallow source excitations were represented by 43 three component accelerograms recorded in Bulgaria, Italy, Turkey and Japan. The Vrancea excitations are represented by 9 three component accelerograms recorded in Bulgaria and Rumania during the 1977, 1986 and 1990 Vrancea earthquakes. The equivalent number of cycles is determined according to he Seed's procedure (1975). The results are summarized below:

Local sources

Equivalent number of cycles
 Mean value: 5.778
 Standard deviation 3.006
 Minimum value: 1.57
 Maximum value: 16.63

Fare field sources

Equivalent number of cycles
 Mean value: 10.34
 Standard deviation 6.08
 Minimum value: 2.82
 Maximum value: 30.62

The multiple deterministic analysis is based on the LHCED procedure. There are 10 samples generated and analyzed for 3 seismic levels (annual probability of exceedance 10^{-3} , 10^{-4} and 10^{-5}). The generation is done on the following key parameters (table 5.2):

For each set of variables the Seed's method for liquefaction analysis is applied deterministically for three levels of seismic excitation. The seismic levels correspond to annual probability of exceedance 10^{-3} , 10^{-4} and 10^{-5} . The seismic hazard curve for maximum acceleration is the one presented for case 2 (fig. 5.2). In order to achieve better accuracy the layer 3 and 4 (where liquefaction is expected) are further subdivided in thinner layers (usually 0.5m thick). For each layer the central factor of safety and the corresponding standard deviation is computed for each seismic level. The conditional probability of failure is computed assuming that the resistance and loading are log-normally distributed. The computed conditional probabilities are presented in table 5.3.

Table 5.2. LHCED generated parameters

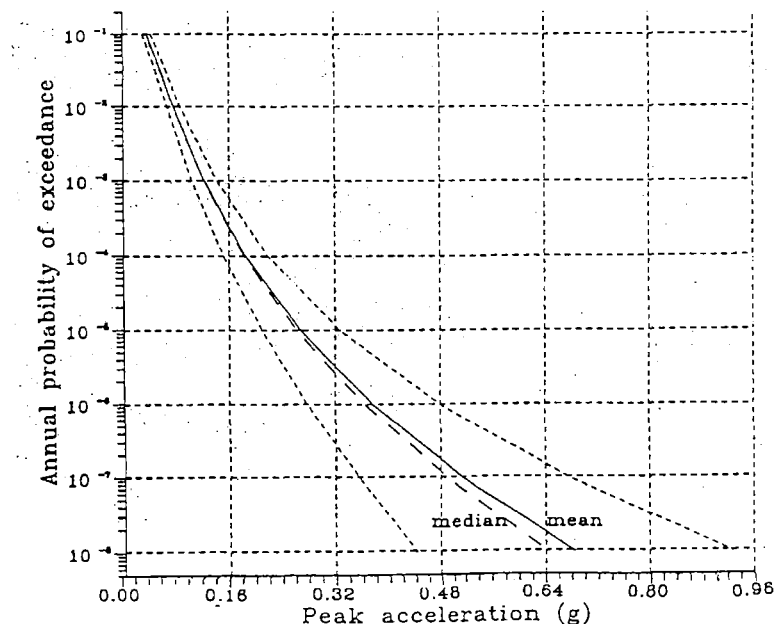
Parameter / Generation No	1	2	3	4	5	6	7	8	9	10
Thickness of layer 1	8.98	10.03	9.76	8.69	10.43	9.39	9.1	9.15	9.66	9.31
Thickness of layer 2	2.89	2.68	3.12	2.96	3.25	3.09	3.15	3.31	3.03	3.60
Thickness of layer 3	1.34	3.00	2.36	1.77	1.93	1.65	0.90	2.29	1.57	1.30
Thickness of layer 4	2.02	3.45	1.66	2.38	2.51	2.78	1.97	2.94	5.05	3.29
Weight density of layer 1	2.02	2.07	2.06	2.06	2.02	2.04	2.00	2.05	2.04	2.03
Weight density of layer 2	2.09	2.12	2.11	2.11	2.09	2.10	2.08	2.10	2.10	2.10
Weight density of layer 3	1.64	1.62	1.64	1.66	1.63	1.65	1.67	1.69	1.66	1.65
Weight density of layer 4	1.60	1.67	1.65	1.71	1.67	1.68	1.59	1.63	1.66	1.63
Underground water level ^{*)}	28.95	28.60	29.81	29.14	29.21	29.34	29.00	28.82	29.57	30.02
Equivalent cycles (10 ⁻³)	2.44	3.58	3.25	2.18	4.10	2.85	2.98	2.60	3.15	2.77
Equivalent cycles (10 ⁻⁴)	7.48	5.59	9.99	8.25	11.69	9.68	10.38	12.52	8.95	17.3
Equivalent cycles (10 ⁻⁵)	10.75	16.79	8.67	12.46	14.63	23.24	20.49	19.15	13.40	27.63
Max. acceleration (10 ⁻³)	0.10	0.12	0.10	0.11	0.12	0.14	0.13	0.13	0.11	0.15
Max. acceleration (10 ⁻⁴)	0.15	0.19	0.14	0.16	0.17	0.21	0.20	0.23	0.24	0.17
Max. acceleration (10 ⁻⁵)	0.20	0.27	0.22	0.18	0.26	0.33	0.28	0.35	0.31	0.25
Relative density of layer 3	42.02	54.22	39.05	46.59	49.92	60.22	57.04	55.62	70.85	47.69
Relative density of layer 4	32.92	44.00	36.37	28.92	41.80	54.77	45.47	58.20	50.45	40.32
Experimental 3-axial soil resistance: eq. $Y=Ax^B$ B=-0.16; A=.....	0.39	0.45	0.49	0.36	0.51	0.42	0.43	0.40	0.45	0.41

*) Underground water level is relative to sea level, the site level is +35.00m.

Table 5.3 Conditional probability of failure due to liquefaction of layers (sub-layers) 3 and 4

Layer No	Level 1 (10 ⁻³)	Level 2 (10 ⁻⁴)	Level 3 (10 ⁻⁵)
3.1	1.78E-10	5.07E-02	5.96E-01
3.2	2.24E-10	5.33E-02	6.05E-01
3.3	2.06E-10	5.51E-02	6.11E-01
3.4	2.34E-10	5.71E-02	6.17E-01
4.1	2.62E-10	5.81E-02	6.21E-01
4.2	2.59E-10	5.69E02	6.23E-01

Fig. 5.2 Hazard curves, mean, median, 15 and 85 percentiles



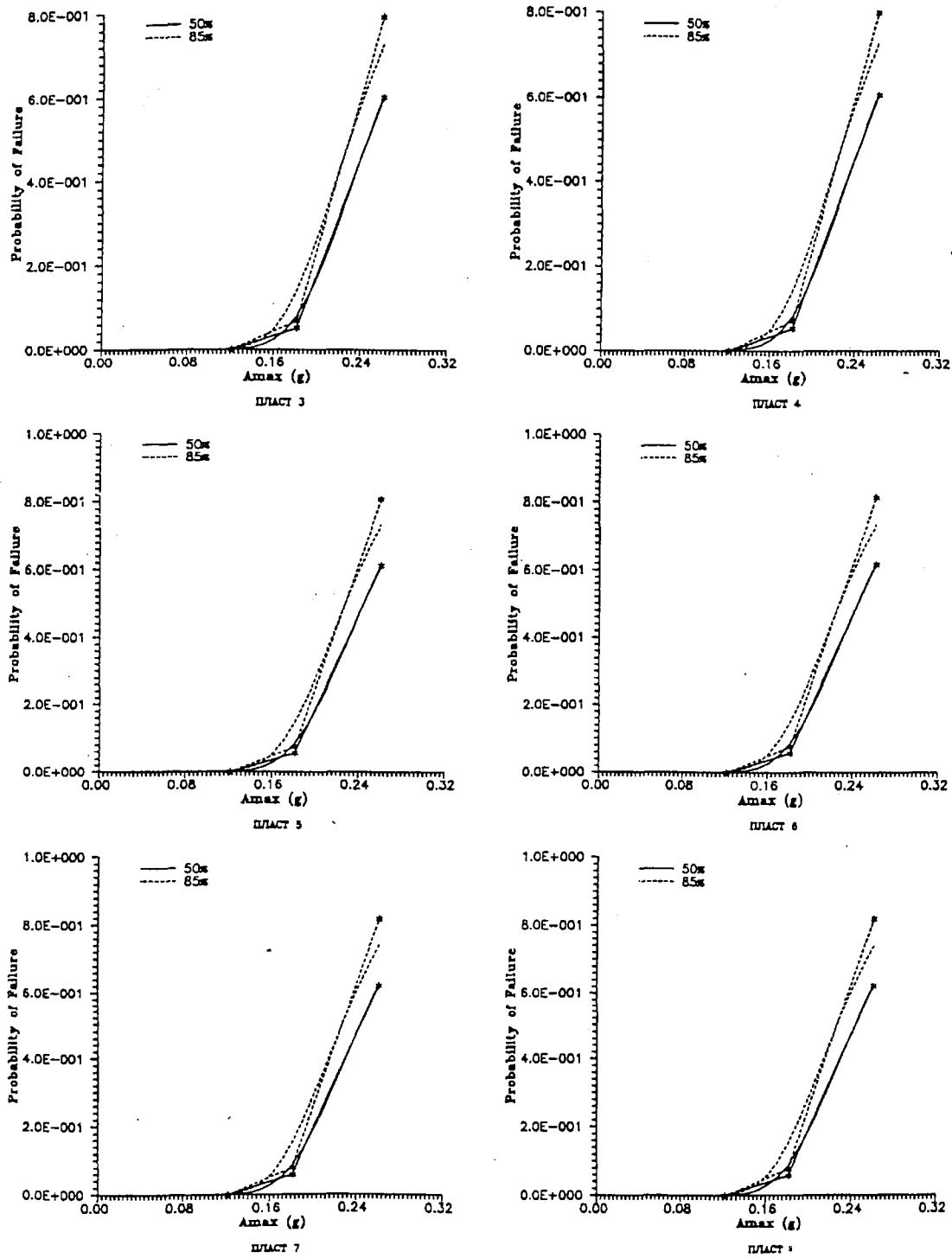


Fig. 5.3 Fragility curve generated by interpolation and extrapolation of the results for each layer

Regional Workshop on External Events PSA, 6-10 November 2000, Sofia

Based on those conditional probabilities a fragility curve is generated by interpolation and extrapolation of the results for each layer (sub-layer), fig. 5.3. The fragility than is convoluted by the hazard curve and the probability of failure due to liquefaction for each layer (sub-layer) is determined.

Table 5.4. Probability of failure due to liquefaction of layers 3 and 4

Layer No	Probability
3.1	6.71E-05
3.2	6.89E-05
3.3	6.98E-05
3.4	7.07E-05
4.1	7.18E-05
4.2	7.19E-05

6. Conclusions

The tools usually applied for probabilistic safety analyses of critical structures could relatively easily be adopted to ordinary structures. The key problems are the seismic hazard definitions and the fragility analyses. The fragility could be derived either based on scaling procedures or on the base of generation. Both approaches have been presented in the paper.

After the seismic risk (in terms of failure probability) is assessed there are several approaches for risk reduction. Generally the methods could be classified in two groups. The first group comprises the methods for monitoring and control. Generally their aim is to collect additional information and based on that to improve assessments. The second group of measures is the engineering. The engineering includes the repair, strengthening and upgrading of the investigated systems. In all cases the risk assessment is a power tool for decision taking.

7. References

- Ang, A. & Tang, W. 1984. Probability concepts in engineering planning and design. Vol. 2. Decision, risk and reliability. John Wiley & Sons.
- Bolotin, V. 1979. Random vibrations of elastic systems. Moscow (in Russian).
- Borges, J.F. & Kastaneta, M. 1971. Structural safety. Lisbon. *LNEC*.
- Cornell, C. 1968. Engineering seismic risk analysis. *BSSA*. Vol.5
- Franzini, J., McCann, M. & Shah, H. 1984. Application of probabilistic risk analysis to the safety of dams. *8WCEE*. Vol. 7. San Francisco.
- Iman, R.L. & Conover, W.J. 1981. Latin Hypercube sampling program. Short course on sensitivity analysis techniques. Texas Technical University.
- Kostov, M. et al. 1994. Report: Probabilistic assessment of the seismic safety and risk of Chaira dam structure. Vol.2. *NEK*.Sofia.
- Kostov, M. et al. 1995. Seismic PSA of Kozloduy 3 NPP, Report, Vo l to.3. *Risk Engineering*, Sofia.
- Kostov, M. et al. 1997. Seismic PSA of Kozloduy 2 Report: Vol.3. *Risk Engineering*, Sofia.
- Lomnitz, C. & Rosenblueth, E. 1976. Seismic risk and engineering decisions. Elsevier.
- Murzeweski, J. 1974. Sicherheit der baukonstruktionen. VEB f. Bauwesen. Berlin.
- NISA II. 1992. Computer code. User manuals. Engineering Mechanics Research Corporation. Michigan.
- Norms for design of buildings and structures in earthquake regions. 1987. Sofia (in Bulgarian).
- Norms (SNiP 2.06.85). 1986. Concrete and reinforced concrete dams. Moscow (in Russian)
- NUREG/CR-2300. 1983. A guide for the performance of the probabilistic risk assessment for nuclear power plants.